A Hybrid Approach to Model the Temperature Effect in Tire Forces and Moments

Bibin S and Ashok Kumar Pandey

Department of Mechanical and Aerospace Engineering, IIT Hyderabad, Kandi, Sangareddy – 502285, India

(Accepted form of the paper as on 19/11/2016 in SAE Journal of Passenger Car – Mechanical Systems: Paper no. 15JPCM-0109,

Abstract

Tire is an integral part of any vehicle which provides contact between the vehicle and the surface on which it moves. Forces and moments generated at the tire-road interaction imparts stability and control of motion to the vehicle. These forces and moments are functions of many variables such as slip, slip angle, contact pressure, inflation pressure, coefficient of friction, temperature, etc. This paper deals with the effect of temperature on the lateral force, the longitudinal force and the self-aligning moment. The analysis is done at different tire surface temperatures such as 20^{o}C, 40^{o}C, and 60^{o}C. Since the experimental set up with the mounted tire is complex and expensive, we use a hybrid approach in which we take the results from the experiments done by the researchers on a sample piece of tire rubber at various temperatures. Then, we do the steady state analysis in ABAQUS considering the variation of coefficient of friction, slip speed and the elastic modulus of rubber with temperature. The steady state numerical results from ABAQUS at different surface temperatures are compared with the modified PAC2002 tire model to capture the temperature effect. After validating the variations of steady state forces and moments from ABAQUS with the modified PAC2002, we use these steady state tire models to do the transient analysis in order to capture the effect of temperature on the transient response of tire forces and moments for different driving conditions of acceleration, braking and double lane change using MSC ADAMS/CAR.

Introduction

A vehicle tire is one of the most vital parts in a vehicle dynamic system. Designing, modeling and fabrication of tires depends on many known as well as uncertain factors as they have to support vehicle weight, provide cushioning effect to surface irregularities, provide sufficient traction for driving and braking, and provide steering control and directional stability. To analyze various effect of tires on the performance of vehicle, most of the tire related effects can be captured in terms of longitudinal force, lateral force, and self-aligning moment. However, accurate computation of the tire forces and moments, and their dependence on various factors such as tire temperature, inflation pressure, contact pressure, the rolling surface, vehicle path, etc., are difficult to predict. In this paper, we focus on the modeling of temperature effect on the tire forces and moment under the acceleration, braking, and lane change conditions of a moving vehicle.

To model the coupled effect of various factors on forces and moments, there exist mainly three classes of modeling techniques, phenomenological/analytical model, empirical model, and numerical models. Initial development of analytical models were mainly based on different simplifications of the tire behavior such as the string based tire models, ring based tire models, and beam-on-elastic foundation based tire models [1,2]. Most of these tire models consider the tread as a pre-stressed string or a ring and the sidewalls as elastic foundations supporting the tread structure. Loo [1] developed an analytical tire model based on the flexible ring under tension with radially arranged linear springs and dampers to represent the tread band of the tire. The developed model was used to characterize the vertical load displacement of tire and its free rolling resistance. Allen et al. [3] mentioned the importance of coupling the tire model with vehicle operating condition. Rotta [4] employed a circular membrane model to represent the sidewall softening effect to analyze the deformation of a tire on a flat surface. To further improve the flexible ring type tire model, Rhyne and Cron [5] proposed the inclusion of bending and shear deformations. Although, these analytical models (also called as phenomenological models) have proved to be valuable to study the general dynamic behavior of tires, they are difficult to be used as a design tool for the tire encompassing various effects. Consequently, many tire companies specify the tire parameters with respect to an empirical tire model, known as the magic formula. The parameters associated with the magic formula can be found by comparing its value with experimental results. Pacejka [6] and his colleagues have established such magic formulas based on measurement data to predict the longitudinal force, cornering force and aligning moment under different loading conditions.

To capture the tire deformation and its coupling effect with road surface, finite element modeling or FEM, of tire were introduced in early 1970 [7]. As FEM formulation and computer speed improved, more accurate FEM models were obtained. Ridha [8] developed a homogeneous tire-road model using three dimensional finite elements. Later, the effective use of three dimensional elements was described by Chang et al [9]. To include the surface effect accurately, Faria et al [10] included contact region in the modeling. Pottinger compared stress distribution of solid and pneumatic tires in the contact region. Danielson et al [11] analyzed three dimensional tire models in cylindrical coordinate system to obtain the forces. Luchini and Popio [12] employed the transient dynamic rolling analysis to obtain the time-histories of strains including the rolling effect. To include the thermal effect, Cho et al [13] predicted the rolling resistance and the temperature distribution of a three dimensional periodic patterned tire. Based on the iterative method, they modeled the coupled effect of hysteresis loss associated with viscoelastic rubber element and the temperature. They concluded that the rolling resistances as well as peak temperature rise are strong function of tire tread pattern. Tang et.al [14] developed a finite element approach to compute the temperature field of a steady-state rolling tire and track using 3D thermal analysis software RADTHERM and FEM software ABAQUS

under different loading and velocity conditions. They found that the temperature fields changes due to change in rolling as well as loading conditions. However, they did not describe the corresponding effect on the forces and moment of tire. In order to compute tire forces and moments, Korunovic et al [15] developed FEM model to study the variation of rubber friction with slip speed and contact pressure without considering temperature. They also compared the numerical results with experimental results. Bibin et al [16] used FEM and incorporated the variation of rubber friction with slip speed at the contact point by using the experimentally measured value from the literature. They showed the variation of tire forces and moments for a given tire pressure and normal load. However, the influence of temperature on forces and moments were not discussed.

To experimentally analyze the effect of temperature on tire forces and moment, Higgins et al [17] investigated the friction process of styrene butadiene rubber which is a standard tire rubber material. To perform the experiments, they used a model tire rubber compound consisting of 46 % styrene/butadiene. Subsequently, they obtained the variation of elastic modulus of tire material with temperature using Tritec 2000 DMA (Dynamic Mechanical Apparatus) system as shown in Fig. 1. Such variation can be considered directly into the material property of tire during finite element simulation. To experimentally understand the variation of coefficient of friction with temperature, Persson [18] studied the variation of the coefficient of friction of a tire tread rubber block sliding on a hard substrate with temperature due to local heating. Based on his experiments, he described the variation of friction with temperature for a particular slip velocity, and then also explained the variation of coefficient of friction with sliding velocity for a particular temperature T=**18**℃. Assuming that the profile of coefficient of friction verses slip velocity remains similar at all temperatures and using the values of the coefficient of frictions versus temperature at a particular slip velocity, we have extrapolated the variation of coefficient of friction with sliding velocities at temperatures T=**20**℃, **40**℃, and **60**℃, respectively, as shown in Fig. 2. Angrick et al. [19] performed experiments to study the dependence of the cornering stiffness, relaxation length, and lateral coefficients of friction on either core or surface temperature of tire.

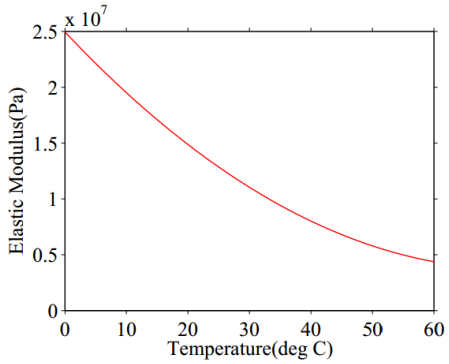

Figure 1: Variation of elastic modulus with temperature [16]

In a nutshell, while the analytical model are limited in capturing various factors associated with the changes in tire material with temperature, etc., the finite element based numerical methods are rarely used to do full vehicle dynamic analysis. As full vehicle dynamics requires multibody analysis of different components of vehicle subjected to any change in operating conditions, the modification of empirical model based on magic formula have been explored. Mizuno et al [19] included temperature effect in magic formula by including additional terms associated with the friction and specific heat and compared the computed lateral force with experiments. Recently, Singh and Shivramakrishnan [20] modified

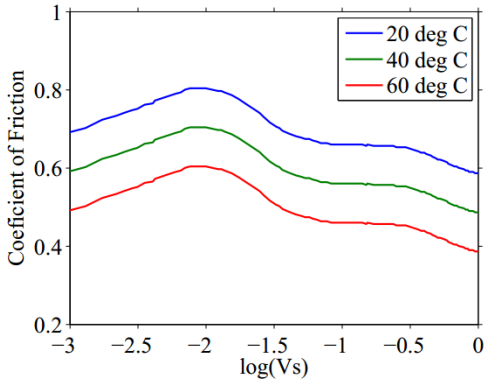

Figure 2: Variation of the coefficient of friction with temperature at different temperatures

the terms associated with cornering stiffness and peak grip level in magic formula to include the influence of temperature, pressure, and normal load. They also compared the results with experimental values. As there may be many limitations for considering various factors in experiments, the above modification in the magic formula should also be compared with corresponding numerical model using FEM. Therefore, we develop FEM model to include the influence of temperature on tire forces and moment by modifying the elastic properties as well as coefficient of friction from Figs. 1 and 2. Subsequently, we use the modified magic formula given by Mizuno et al [20] and compute the related constants based on numerical results. Finally, to discuss the performance of modified tire model under the influence of temperature on the driving, braking, and lane change conditions, we perform transient analysis in multibody software, ADAMS.

The Magic Formula PAC2002 Tire Model with Temperature effects

In this section, we present mathematical details of empirical model, also known as magic formula or PAC2002 model [6], to capture the steady state tire forces and moments under the influence of temperature [20]. The magic formula to find the steady state forces and moments are expressed as [6]

$$Y(X) = y(x) + S_v \quad (1)$$

$$y(x) = D\sin[C\arctan\{Bx - E(Bx - \arctan(Bx)\}] \quad (2)$$

$$x = X + S_h \quad (3)$$

where, *D*, *C*, *B*, *E* are the main parameters of the magic formula. These parameters are tuned to fit the magic formula curve with the tire measurement data/numerical results. The values of these parameters give an idea about the tire-road interaction surface, properties of tire, etc. For example, the parameter D is the peak factor, which gives an idea of the coefficient of friction at the interaction. C is the shape factor, B is the stiffness factor, E is the curvature factor. The product

of parameters BCD, which is the slope of magic formula curve, gives the stiffness of the tire. (S_h) is the vertical shift and (S_v) is the horizontal shift of the curve due to side slip in the horizontal and vertical directions, respectively. We use this formula to compute the longitudinal force (F_x), lateral force (F_y) and self-alignment moment (M_z). Table 1 presents the relationship between dependent variable, Y(X), and independent variable, *X*, of magic formula to compute the tire forces and moment.

Table 1: Independent and Dependent Variables of Magic Formula.

Independent quantity (*X*)	Longitudinal slip(k)	slip angle(α)	slip angle(α)
Dependent quantity(Y)	Longitudinal Force (F_x)	Lateral Force (F_y)	Pneumatic trail(t) ($M_z = -t \times F_y$)

To include more variables in magic formula, Pacejka modified the basic form of the magic formula to obtain PAC2002 tire model by defining new parameters which captures the effect of camber angle, etc. [6]. Subsequently, other researchers modified PAC2002 model to include the effect of pressure, temperature, etc. [20, 21]. In this paper to capture the temperature related effect on the longitudinal force, lateral force and cornering moment, we use the modified model proposed by Mizuno et al [20] which was obtained by modifying PAC2002 model to find lateral force. In the subsequent section, we present the details of the modified PAC2002 model and describe the procedure to include temperature effects.

Lateral Force at Pure Slip

Lateral force, F_y, is developed due to the existence of a side slip angle under the cornering condition. The side slip angle or slip angle (α) is defined as the angle between the direction of travel of the tire and the direction of wheel plane. The temperature effects on lateral force are modeled under the assumptions that the lateral force varies proportional to the tire surface temperature, and its maximum value is dependent on different proportionality constant with respect to the temperature [20]. The expression of lateral force can be written as

$$F_y(\alpha, T) = D_y(T)\sin[C_y \arctan\{B_y(T)\alpha_y - E_y(B_y(T)\alpha_y - \arctan(B_y(T)\alpha_y))\}] + S_{Vy} \quad (4)$$

where,

$$\alpha_y = \alpha + S_{Hy} \quad (5)$$

$$C_y = p_{Cy1}.\lambda_{Cy} \quad (6)$$

$$D_y = \mu_y.F_z.\zeta_2 \quad (7)$$

$$D_y(T) = D_y.\{1 + \frac{\partial \mu}{\partial T}(T - T_m)\} \quad (8)$$

$$\mu_y = (p_{Dy1} + p_{Dy2}.df_z).(1 - p_{Dy3}.\gamma^2)\lambda_{\mu y} \quad (9)$$

$$E_y = (p_{Ey1} + p_{Ey2}.df_z)(1 + p_{Ey5}\gamma 2 - (p_{Ey3} + p_{Ey4}.\gamma_y).sgn(\alpha_y)).\lambda_{Ey} \quad (10)$$

$$B_y(T) = \frac{K_y(T)}{C_y.D_y(T)} \quad (11)$$

$$K_y(T) = Ky.\{1 + \frac{\partial C_p}{\partial T}(T - T_m)\} \quad (12)$$

$$K_y = p_{Ky1}.F_{z0}.\sin[2\arctan(\frac{F_z}{p_{Ky2}.\lambda_{Fz0}.F_{z0}})].(1 - p_{Ky3}.|\gamma_y|).\zeta_3.\lambda_{Ky}.\lambda_{Fz0} \quad (13)$$

$$S_{Hy} = (p_{Hy1} + p_{Hy2}.df_z)\lambda_{Hy} + p_{Hy3}.\gamma_y.\zeta_0 + \zeta_4 - 1 \quad (14)$$

$$S_{Vy} = F_z.\{(p_{Vy1} + p_{Vy2}.df_z)\lambda_{Vy} + (p_{Vy3} + p_{Vy4}.df_z).\gamma_y\}.\zeta_4.\lambda_{\mu y} \quad (15)$$

$$\gamma_y = \gamma.\lambda_{\gamma y} \quad (16)$$

where, T_m is the ambient average tire surface temperature, D_y, E_y, K_y, etc., are the parameters of steady state tire lateral force model at T_m. D_y (T), B_y (T) and K_y (T) are the parameter values at any temperature T. The rate of change of the peak parameter D_y (T) and cornering stiffness parameter K_y (T) with temperature can be correlated with the corresponding change in the coefficient of friction and the specific heat, respectively, as [20]

$$\frac{\partial \mu_y}{\partial T} = \frac{d(D_y(T))/dT}{D_y} \quad (17)$$

$$\frac{\partial C_p}{\partial T} = \frac{d(K_y(T))/dT}{K_y} \quad (18)$$

where, $d(D_y(T))/dT$ is equal to the gradient of peak value of lateral force with respect to temperature. Since the coefficient of friction, μ_y, is correlated with change in peak value due to change in temperature, we capture the effect of temperature change in numerical modeling by varying the coefficient of friction, μ_y, corresponding to different temperatures. Taking μ_y from the experimental results [18] and developed empirical relation at different temperature as shown in Fig. 2, we compute the peak value of lateral force under the load of 4 kN from the numerical results using ABAQUS. Although, we will present the detail discussion on numerical modeling later, we present the variation of peak value of lateral force at different temperatures in Table 2. Consequently, the value of $d(D_y(T))/dT$ is found as 20.56 N. Similarly, to compute $d(K_y(T))/dT$, which is defined as the rate of change of lateral force with respect to change in temperature corresponding to the slip angle of $\pm 1^o$[19], we numerically compute lateral forces for $\mu_y(T)$ corresponding to different temperatures when the slip angle is fixed at $\pm 1^o$ as mentioned in Table 3. After computing the gradient of forces with respect to equivalent change in temperature for $+1^o$ and -1^o separately, we take average value of the gradient of K_y (T). The value of $d(K_y(T))/dT$ is found as 7.78 N/deg. In the subsequent sections, we compute describe the computation of longitudinal force and aligning torque by following the same approach.

Table 2: Variation of Peak Lateral Force with Temperature from ABAQUS.

Temperature (degree Celsius)	Peak value of Lateral force(N) (for -ve slip angles)	Peak value of Lateral force(N) (for +ve slip angles)

20	-2615.65	2393.38
40	-2203.61	1977.23
60	-1799.22	1565.01

Table 3: Variation of Lateral Force at α = $\pm 1^0$ corresponding to Different Temperatures obtained from ABAQUS.

Temperature (degree Celsius)	Lateral force(N) (at $\alpha = -1^o$)	Lateral force(N) (at $\alpha = +1^o$)
20	-1247.28	1026.01
40	-1114.58	890.867
60	-945.005	706.167

Longitudinal Force at Pure Slip

To compute longitudinal force, we first define the slip speed or slip velocity at the tire-road interface which produces shear force in the longitudinal direction called as longitudinal force, F_x. This slip velocity is due to the speed difference between tangential velocity of tire at the contact patch ($R_e\omega_w$) and the velocity of the vehicle ($R_0\omega_w$). The slip ratio (k) of the slip velocity to the velocity of the vehicle can be expressed as

$$k = -\frac{V_x - R_e\,\omega_w}{V_x}, \quad (19)$$

$$V_x = R_0\omega_w \quad (20)$$

where, V_x is the longitudinal velocity of the vehicle, R_e is the effective rolling radius and ω_w is the angular velocity of the wheel. Following the similar procedure as mentioned by Mizuno et al [20] to obtained modified PAC2002 model for lateral forces only, here, we also modify the PAC 2002 model to study the effect of temperature on longitudinal forces and self-alignment moment. The modified PAC2002 model for longitudinal force can be written as,

$$F_x(k,T) = D_x(T)\sin[C_x\arctan\{B_x(T)\,k_x - E_x(B_x(T)\,k_x - \arctan(B_x(T)\,k_x))\}] + S_{Vx} \quad (21)$$

where,

$$k_x = k + S_{Hx} \quad (22)$$

$$C_x = p_{Cx1}.\lambda_{Cx} \quad (23)$$

$$D_x = \mu_x.F_z.\zeta_1 \quad (24)$$

$$D_x(T) = D_x.\{1 + \frac{\partial\mu_x}{\partial T}(T - T_m)\} \quad (25)$$

$$\mu_x = (p_{Dx1} + p_{Dx2}.df_z).\lambda_{\mu x} \quad (26)$$

$$E_x = (p_{Ex1} + p_{Ex2}.df_z + p_{Ex3}.df_z^2).(1 - p_{Ex4}.sgn(k_x)).\lambda_{Ex}$$

$$B_x(T) = \frac{K_x(T)}{C_x.D_x(T)} \quad (27)$$

$$K_x = F_z.(p_{Kx1} + p_{Kx2}.df_z).(exp(p_{Kx3}.df_z)).\lambda_{Kx} \quad (28)$$

$$K_x(T) = K_x.\{1 + \frac{\partial C_p}{\partial T}(T - T_m)\} \quad (29)$$

$$S_{Hx} = (p_{Hx1} + p_{Hx2}.df_z)\lambda_{Hx} \quad (30)$$

$$S_{Vx} = F_z.(p_{Vx1} + p_{Vx2}.df_z)\lambda_{Vx}.\lambda_{\mu x}.\zeta_1 \quad (31)$$

$$\gamma_x = \gamma.\lambda_{\gamma x} \quad (32)$$

where, T_m is the ambient average temperature of tire surface. The steady state analysis of tire forces without elevated temperature is done at this temperature. D_x, E_x, K_x are the parameters of steady state lateral force of tire at a given temperature T_m. $D_x(T)$, $B_x(T)$ and $K_x(T)$ are the parameter values when the effect of tire surface temperature is included. Like previous section, taking

$$\frac{\partial\mu_x}{\partial T} = \frac{d(D_x(T))/dT}{D_x}, \quad (33)$$

$$\frac{\partial C_p}{\partial T} = \frac{d(K_x(T))/dT}{K_x} \quad (34)$$

where, $d(D_x(T))/dT$ is equal to the gradient of peak value of longitudinal force with respect to temperature. The value can be calculated from the numerical results using ABAQUS as described in the previous section. Table 4 shows the variation of peak value of longitudinal force at different temperatures. Taking the average value of the gradient on both positive (clockwise) and negative (counter-clockwise) slip ratio, $d(D_x(T))/dT$ can be obtained. $\partial\mu_x/\partial T$ can also be taken from the variations of friction with temperature as shown in Fig.2.

Table 4: Variation of Peak Longitudinal Force with Temperature from ABAQUS

Temperature (degree Celsius)	Peak value of Longitudinal force (N) (for -ve slip)	Peak value of Longitudinal force (N) (for +ve slip)
20	-2624.48	2609.21
40	-2214.65	2207.13
60	-1807.15	1798.49

Table 5: Longitudinal Force (at k= 1) at different Temperatures from ABAQUS.

Temperature (degree Celsius)	Longitudinal force (N) (at k=-1)	Longitudinal force (N) (at k=+1)

20	-2375.011	2385.912
40	-1974.855	1990.495
60	-1574.715	1589.279

Similarly, $d(\mathrm{K_x}(\mathrm{T}))/dT$ is taken as the gradient of longitudinal force at slip ($k = \pm 1$) with respect to temperature as mentioned in Table 5. It is clear from the profile of steady state longitudinal curves that the variation of longitudinal forces at k = .3 is same as that at k = 1. Therefore, as we do not have the coefficient of friction corresponding to k=1, we first obtain the variation of longitudinal forces at k=.3 numerically and then assign the same value of force at k=1. In order to find the value of $d(\mathrm{K_x}(\mathrm{T}))/dT$, the longitudinal forces at different temperatures are extracted from ABAQUS for a slip of +1 and -1, and then the gradient is calculated for both cases, separately. The mean of the two gradients gives the value of $d(\mathrm{K_x}(\mathrm{T}))/dT$.

Self-Aligning Moment at Pure Slip

During cornering, the lateral force acting at the tire-surface interface is often asymmetric about the wheel plane. Consequently, it induces a moment or torque, known as self-aligning moment (M_z), about the vertical axis. Such moment tends to rotate the tire so as to minimize the effect of slip angle. The magnitude of the self-aligning moment depends on pneumatic trail t(α) and residual moment, M_{zr}. The pneumatic trail also varies with temperature. Hence, we modify the expression for pneumatic trail t(α,T) and the corresponding moment M_z(T) by including the effect of temperature. The expression for the self aligning moment without the influence of temperature can be written as

$$M_z = -t(\alpha).F_y + M_{zr} \tag{35}$$

and the expression for self-aligning moment considering the temperature effects is expressed as

$$M_z(T) = -t(\alpha,T).F_y(T) + M_{zr} \tag{36}$$

$$t(\alpha) = D_t \sin[C_t \arctan\{C_t\alpha_t - E_t(B_t\alpha_t - \arctan(B_t\alpha_t))\}] \tag{37}$$

$$t(\alpha,T) = D_t(T)\sin[C_t \arctan\{B_t\alpha_t - E_t(B_t\alpha_t - \arctan(B_t\alpha_t))\}] \tag{38}$$

where,

$$\alpha_t = \alpha + \mathrm{S_{Ht}} \tag{39}$$

$$C_t = q_{\mathrm{Cz1}} \tag{40}$$

$$D_t = (q_{\mathrm{Dz1}} + q_{\mathrm{Dz2}}.df_z)(1 + q_{\mathrm{Dz3}}\gamma_z + q_{\mathrm{Dz4}}\gamma_z^2)R.F_{z0}.\lambda_t.\zeta_5 \tag{41}$$

$$D_t(T) = D_t\left(1 + \frac{\partial t_{peak}}{\partial T}(T - T_m)\right) \tag{42}$$

$$E_t = (q_{\mathrm{Ez1}} + q_{\mathrm{Ez2}}df_z + q_{\mathrm{Ez3}}.df_z^2) \tag{43}$$

$$B_t = (q_{\mathrm{Bz1}} + q_{\mathrm{Bz2}}df_z + q_{\mathrm{Bz3}}.df_z^2)(1 + q_{\mathrm{Bz4}}.\gamma_z + q_{\mathrm{Bz4}}|\gamma_z|)\frac{\lambda_{Ky}}{\lambda_{By}} \tag{44}$$

$$S_{Ht} = (q_{\mathrm{Hz1}} + q_{\mathrm{Hz2}}.df_z)(q_{\mathrm{Hz3}} + q_{\mathrm{Hz4}}.df_z).\gamma_z \tag{45}$$

$$\gamma_z = \gamma.\lambda_{\gamma z} \tag{46}$$

The residual moment, M_{zr}, can be expressed as

$$M_{zr} = D_r.\cos[C_r.\arctan(B_r.\alpha_r)].\cos(\alpha) \tag{47}$$

$$\alpha_r = \alpha + S_{Hf} \tag{48}$$

$$S_{Hf} = S_{Hy} + \frac{S_{Vy}}{K_y} \tag{49}$$

$$C_r = \zeta_7 \tag{50}$$

$$D_r = F_z.[(q_{\mathrm{Dz6}} + q_{\mathrm{Dz7}}.df_z).\lambda_r + (q_{\mathrm{Dz8}} + q_{\mathrm{Dz9}}.df_z).\gamma_z].R_0.\lambda_{\mu\gamma} + \zeta_8 - 1 \tag{51}$$

$$B_r = \left(q_{\mathrm{Bz9}}.\frac{\lambda_{Ky}}{\lambda_{\mu y}} + q_{\mathrm{Bz10}}.C_y.B_y\right).\zeta_6 \tag{52}$$

$$C_r = \zeta_7 \tag{53}$$

$$df_z = \frac{F_z - F'_{z0}}{F'_{z0}} \tag{54}$$

$$F'_{z0} = F_{z0} \times \lambda_{Fz0} \tag{55}$$

where, $\partial t_{peak}/\partial T$ is the variation of peak pneumatic trail with temperature. Again, we find its value from the numerical simulation in ABAQUS. From ABAQUS, first, we extract the peak value of self aligning moment at three different temperatures. Then, we find the pneumatic trail by dividing the extracted peak of self-aligning moment with the lateral force for the corresponding slip angle including the temperature related effect. This process is done for positive and negative slip angles. The mean of slope of pneumatic trail versus temperature at positive and negative slip angles gives the value of $\partial t_{peak}/\partial T$.

In the PAC2002 model, F_z and F_{z0} are normal load and nominal load, respectively. p_{Cx1}, p_{Dy2}, q_{Ez3}, etc., are sub parameters which control the variation of main parameters (C_x, D_y, E_t etc) with different conditions such as the variation of load, inclination angle, residual moment, etc. λ_{Cx}, λ_{By} are the scaling factors of main parameters and other inputs of magic formula such as camber angle, μ_y. x, y and z in the suffix indicate that the parameters or sub parameters are associated with the forces along x-direction, y-direction and moment about z-direction, respectively.

The p in the sub parameter denotes the force at pure slip while that with q denotes the moment at pure slip. ζ_i is the reduction factor. Since, turn-slip is neglected for steady state pure slip condition and small camber, the value of ζ_i can be set to 1. R_0 is the unloaded wheel radius. γ is the roll angle or camber angle which is neglected in our analysis.

Steady State Analysis – FEM Approach

In this section, we discuss the finite element modeling, FEM, of the tire and compare the FEM results with modified PAC2002 model. First, we model a tire and the road on which tire rolls, and then apply loads and boundary conditions. Then, for a given motion, we compute the forces and moments at the tire-road interaction. These forces and moments from ABAQUS are compared with the results from modified PAC2002 model considering temperature effects. Finally, these models are used for transient analysis which are described later in next section. The details of the finite element model are explained as follows.

FEM Modeling

The FEM modeling and analysis of tire is done using ABAQUS based on the approach as mentioned in [16] and [22]. We model different components such as carcass, sidewall, belt, tread, membrane belt, etc., with appropriate materials and elements as shown in Figure 3. Rubber is used to model tread and sidewalls, whereas fiber reinforced rubber composite is used to model carcass and belt. The rubber used in the tire is modelled as an incompressible hyperelastic material model which includes a time domain viscoelastic component and the fiber reinforced in the fiber reinforced rubber composite is modeled as a linear elastic material. The time-domain viscoelastic component is defined by a Prony series expansion of the relaxation dimensionless modulus with relaxation time of 0.1. This component is employed to incorporate the stress relaxation with respect to the time at constant strain. Long term parameter is used with hyperelastic model to incorporate long term behavior of the rubber. The variation of elastic modulus of rubber with temperature is also considered and the variation is taken from the experiment done by Higgins et al [17] on a sample piece of tire rubber.

The half section of the three dimensional model is first generated from axisymmetric model. The belts and ply are modeled with rebar in surface elements embedded in continuum elements (rubber). After axisymmetric modelling, the cross section is revolved about the rotational symmetry axis (wheel axle). Then, this partial three dimensional model is reflected about the plane normal to the axis of revolution to obtain the three dimensional model as shown in Figure 3(a). The sectional component of tire is also shown in Figure 3(b). The road is assumed as an analytical-rigid surface. The hard contact is used to model the contact between the tire and the road since the contact relationship minimizes the penetration of slave surface (tire) into the master surface (road) at the constraint location. Instead of giving a vertical load (negative-z direction) on the tire axle, a load is applied on the road in upward (positive-z) direction. Finally, to consider the inflation pressure, we apply uniform pressure of 220 kPa in the inner surface of the tire. Under the influence of such pressure, the tire experiences circumferential deformation which creates three dimensional stress field with non-varying stresses in the circumferential direction.

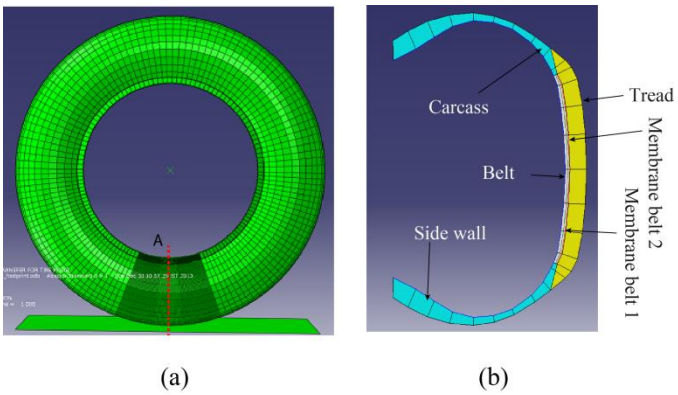

Figure 3: (a) Three-dimensional tire model in ABAQUS, (b) A typical tire section with different elements.

The steady state rolling analysis of the tire is done based on Coupled Eulerian Lagrangian (CEL) formulation. In this formulation, the tire rotation and movement are considered in Eulerian frame, and the deformation is considered in Lagrangian frame. Consequently, the steadily moving contact problem is transformed into a pure spatially dependent simulation. In this formulation, contact region (40^o) is more important and is meshed with more number of linear solid elements (C3D8H and C3D6H). Since, the contact region has dense nodes, and each element may be assumed to undergo a small deformation, we use linear elements in order to reduce the computation time. Rest of the tire section (i.e., 320^0) is modeled with cylindrical elements (CCL12H and CCL9H) with relatively sparse nodes to cover large sectors with small number of elements.

Steady State Rolling Analysis

We perform steady state analysis of the tire (based on CEL formulation) under a vertical load of 4 kN acting along the tire axis. In this analysis, the ground velocity of the tire is taken as 10 km/h (2.7778 m/s). The coefficient of friction (μ_r) of the rubber tire at the tire-road interaction are dependent on the temperature and slip speed. As discussed earlier, we take the variation of friction coefficient from the experiments done by Persson [18] on a tire rubber sample at various temperatures and slip speeds. We incorporate these coefficient of friction values for the FEM modeling and analysis in ABAQUS. The variation of elastic modulus of tire rubber with temperature is also taken into account from the experiments done by Higgins et.al [17] as shown in Table 2. The lateral and longitudinal forces are the frictional shear forces acting on the contact area and self-alignment moment is the product of the resultant of the lateral force and the offset of the line of action of resultant from the center point of the contact region at zero cornering condition.

Steady State Lateral Force

In order to extract the lateral force from ABAQUS, we have to consider the variation of coefficient of friction with lateral slips and temperature. As discussed earlier, we make use of the temperature dependent elastic modulus values and the coefficient of friction values from the experiments done by Persson [18] on a sample piece of tire rubber at different temperatures as mentioned in Table 6 and 7. Table 7 shows the variation of μ verses slip speed at different temperatures.

In this case, the slip speed is the lateral slip speed (V_{sy}) corresponding to each slip angle. The lateral slip speed of a tire taking a turn with a velocity, V, can be expressed as:

$$V_{sy} = V_y = V\sin(\alpha) \qquad (56)$$

Table 6. Elastic modulus of rubber tire at various temperatures.

Sl. No	Temperature (degree Celsius)	Elastic Modulus (Pascal)
1	20	15135612.48
2	40	7943282.347
3	60	4466835.922

Table 7. The coefficients of friction at various temperatures.

Slip angle (α) in degrees	Comp. of vel. in longi. direction (V_x) in m/s	Comp. of vel. in lateral direction (V_y) in m/s	Coeff. of friction at 20^oC μ_{20}	Coeff. of friction at 40^oC μ_{40}	Coeff. of friction at 60^oC μ_{60}
0	2.7778	0	0.6920245	0.5920245	0.4920245
0.5	2.7777	0.0242406	0.6920245	0.5920245	0.4920245
1	2.7774	0.0484794	0.7411473	0.6411473	0.5411473
2	2.7761	0.0969440	0.6779894	0.5779894	0.4779894
3	2.7740	0.1453791	0.6604456	0.5604456	0.4604456
4	2.7710	0.1937699	0.6569368	0.5569368	0.4569368
5	2.7672	0.2421017	0.6569368	0.5569368	0.4569368
7.5	2.7540	0.3625765	0.6429017	0.5429017	0.4429017
10	2.7356	0.4823610	0.6253578	0.5253578	0.4253578
12	2.7171	0.5775384	0.6148315	0.5148315	0.4148315
15	2.6831	0.7189491	0.6007964	0.5007964	0.4007964

In this section, we will first validate lateral force at a given temperature obtained from our FEM model with the experimental results obtained by Mizuno et al [20]. To do the FEM analysis, we need to input the coefficient of friction, μ, corresponding to the tire road interaction. We take μ corresponding to peak lateral force such that $\mu_{peak} = F_{y_{peak}}/F_z$, and then assume its variation as mentioned in Figure 2. The validation is done for two different temperatures when the slip angles vary 0 to $\pm 15^o$. Taking the vertical normal load as 4600N, we show the comparison of FEM results with the experimental results [20] in Figures 4 and 5 corresponding to temperatures of 60° and 28°C. The results show that there is a slight variation of both the results especially in the region of 0 to 5^0. Since the slope of the curve in this region indicates the stiffness of the tire, the difference in results are found due to the negligence of several factors which may become important during the experimentation. It shows that the numerical results over predict the stiffness of the force. In the Figure 4, we only show the variation of force with negative slip angle because Mizuno et al [20] has done the analysis at higher temperatures (60^oC) on negative slip angle. Similarly, we present the variation of force at lower temperature (28^oC) only over positive slip angle in Figure 5 because the experimental results are only available over that range at lower temperature.

From Figures 4 and 5, we notice slight change in the peak lateral forces corresponding to lower temperature due to decrease in the co efficient of friction with increase in temperature. We also observed the difference in the lateral force at around $\pm 15^0$ because we have considered the linear variation of friction with temperature corresponding to a slip speed of 1 m/s. From experiments from Figure 2, it is evident that, at higher temperatures (above 40^o) , the variation the coefficient of friction becomes nonlinear with temperature.

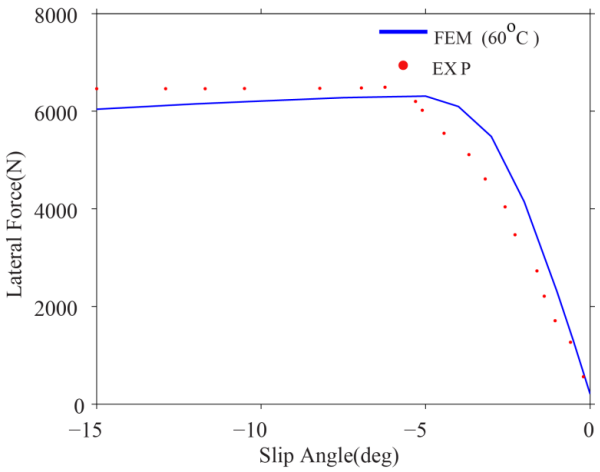

Figure 4: Validation of FEM results with experimental results [?] for negative slip angles, (b)Validation for positive slip angles

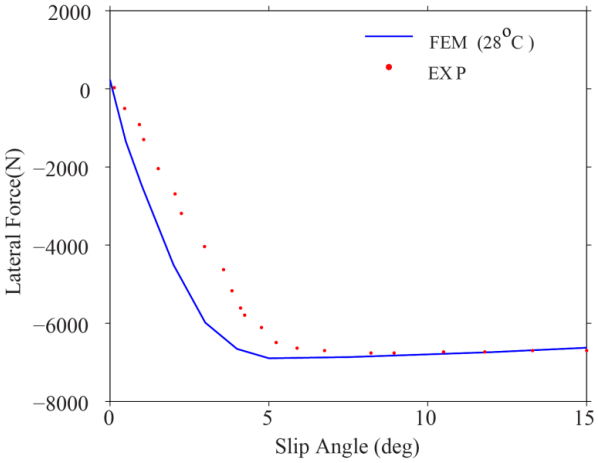

Figure 5: Validation of FEM results with experimental results [?] for positive slip angles

After approximately validating the numerical model with experiments, we do the steady analysis in ABAQUS on a tire under the normal load of 4000N. The coefficient of friction values used for the analysis is extrapolated from the experiments done by Persson [18] on sample piece of tire rubber. Table 7 shows the value of coefficient of friction at different temperatures and lateral slip speed. The steady state lateral forces versus slip angle obtained from FEM at 20º, 40º and 60ºC are shown in Figure 6. Subsequently, we also fit the modified PAC2002 model to identify different parameters based on the numerical results at different temperatures. Figure 6 also present the comparison of FEM and PAC2002 model under the effect of different temperatures.

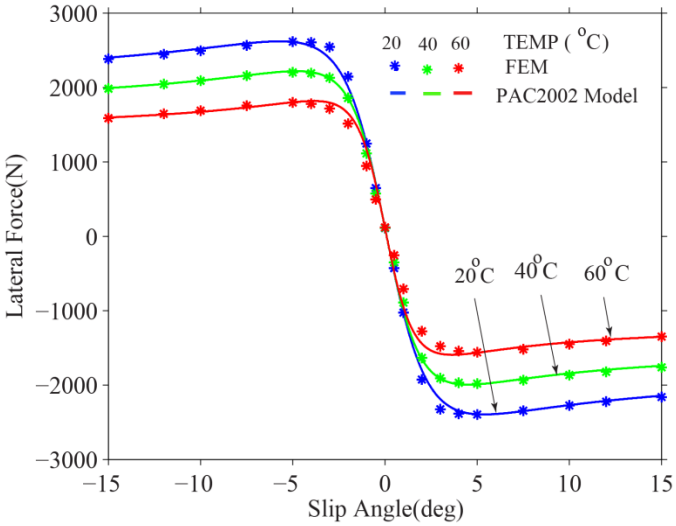

Figure 6: Variation of lateral force versus slip angle at different temperatures - FEM and modified PAC2002 model

Steady State Longitudinal Force

To numerically compute the steady state longitudinal force at different longitudinal slip, we take the velocity of the tire axle as 10km/hr. For the given velocity, we find the effective rolling radius. When the tire rolls under the effect of negligible torque, we find the angular velocity of the tire. Under this rolling condition, the longitudinal force acting on the tire road interaction tends to zero. We terms this condition as free rolling condition which is obtained by trial and error method. The radius corresponding to this free rolling condition is called effective rolling radius. After finding the free rolling condition, longitudinal slip can be given to the tire by giving an angular velocity different from that of the free rolling. The different angular velocity applied to acquire different longitudinal slips are also mentioned in Table 8. Finally, we incorporate the variation of coefficient of friction with longitudinal slips and temperature to extract the longitudinal force. Using the variation of μ as mentioned in Table 8, the steady state longitudinal force obtained from FEM versus longitudinal slips at different temperatures are shown in Figure 7. Subsequently, we also obtain the parameters associated with modified PAC2002 model based on the numerical results shown in Figure 7.

Table 8. Coefficient of friction w.r.t longitudinal slip at different temperatures

Slip (k)	Slip speed (Vs) in m/s	Coe. of fric at 20^oC (μ_{20})	Ang. vel. at 20^oC (ω_{20}) in rad/s	Coe. of fric at 20^oC (μ_{20})	Ang. vel. at 20^oC (ω_{40}) in rad/s	Coe. of fric at 60^oC (μ_{60})	Ang. vel. at 20^oC (ω_{60}) in rad/s
0	0.00000	0.69202	9.01001	0.59202	9.02450	0.49202	9.03130
0.0005	0.00139	0.70255	9.00550	0.60255	9.01999	0.50255	9.02679
0.001	0.00278	0.74816	9.00100	0.64816	9.01548	0.54816	9.02227
0.002	0.00556	0.78325	8.99199	0.68325	9.00645	0.58325	9.01324
0.003	0.00833	0.80431	8.98298	0.70431	8.99743	0.60431	9.00421
0.005	0.01389	0.79378	8.96496	0.69378	8.97938	0.59378	8.98615
0.01	0.02778	0.73062	8.91991	0.63062	8.93426	0.53062	8.94099
0.015	0.04167	0.68852	8.87486	0.58852	8.88913	0.48852	8.89583
0.025	0.06945	0.66395	8.78476	0.56395	8.79889	0.46395	8.80552
0.05	0.13889	0.66045	8.55951	0.56045	8.57328	0.46045	8.57974
0.075	0.20834	0.65694	8.33426	0.55694	8.34766	0.45694	8.35395
0.100	0.27778	0.65343	8.10900	0.55343	8.12205	0.45343	8.12817
0.150	0.41667	0.63588	7.65850	0.53588	7.67083	0.43588	7.67661
0.200	0.55556	0.61834	7.20800	0.51834	7.21960	0.41834	7.22504
0.300	0.83334	0.59378	6.30700	0.49378	6.31715	0.39378	6.32191

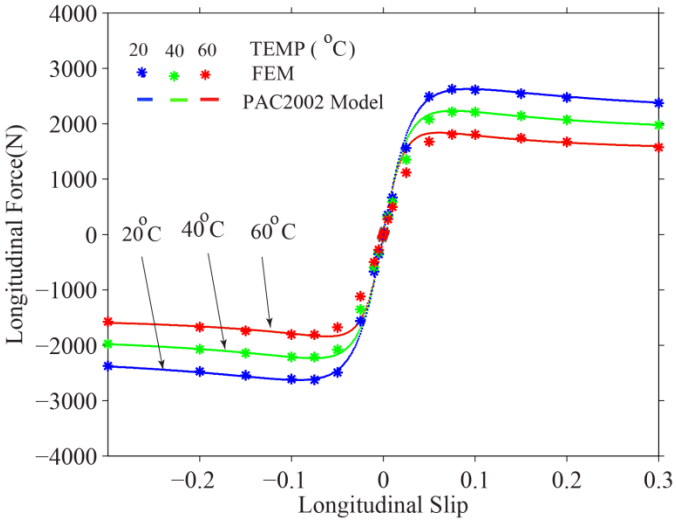

Figure 7: Variation of longitudinal force versus slip ratio at different temperatures-FEM and modified PAC2002 model

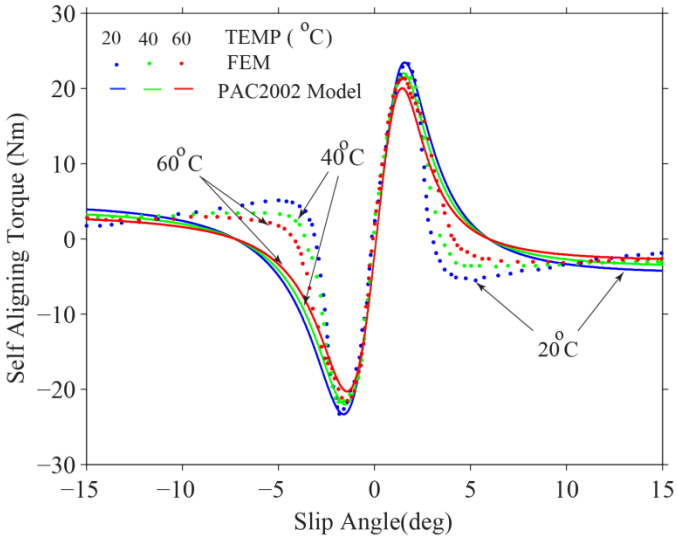

Figure 8: Variation of self-aligning torque versus slip angle at different temperatures - FEM and modified PAC2002 model

Steady State Self Aligning Moment

Since the self-aligning moment is the product of the resultant of lateral force and the pneumatic trail, i.e., $M_z = -t \times F_y$, we consider the effect of temperature on lateral force but the variation of pneumatic trail with temperature is assumed to be negligible. To find the resultant moment due to the lateral force about the center of the contact point, we compute the sum of the product of lateral force (shear force in the lateral direction) at each node with the perpendicular (longitudinal distance) distance of the center of contact point at zero slip to line of action of action of lateral force at corresponding slip angle on that node. The effect of temperature on lateral forces have already been discussed in the previous section. Finally, the steady state self- aligning moments from FEM at three different temperatures (20^oC, 40^oC, 60^oC) versus slip angle are computed and compared with the modified PAC2002 model in Figure 8. The comparison of models show that the PAC2002 model captures the peak location and its variation temperature effectively. The difference in the values after the peak may require further improvement in fitting the data. Additionally, the simplified assumption of lateral stiffness in computing the lateral forces may also lead to some error in numerical results. Therefore, as far as numerical modeling is concern, it may also require little more improvement. Since, our focus in this paper is to analyze the effect of forces and moment under small change in slip angle, we carry out further analysis with the present fitted parameters of PAC2002 model in the next section.

In this section, we have done the steady state analysis to compute the tire forces and moment using in FEM by including the effect of temperature. Subsequently, we tuned the modified PAC2002 model parameters. It has been found out that the variation of forces and moments with temperature from FEM are in agreement with that from the modified PAC2002 model. The next step is to use these steady state models at different temperatures (20^oC, 40^oC, 60^oC) to find the transient forces and moments under the influence of temperature.

Transient Analysis of Forces and Moment under Temperature Effect

This section deals with the study of the effect of temperature on the transient analysis of tire. Experimental determination of transient forces and moments at various temperatures are very complex and expensive. Additionally, it is also difficult to maintain a constant tire-surface temperature while doing the analysis. To overcome these difficulties, we explain a hybrid approach to find these transient forces and moments using ADAMS car model. We will find the transient forces and moments at different temperatures for the three different conditions such as the double lane change (DLC), acceleration and braking by exporting the parameters associated with modified PAC2002 model.

ADAMS Transient Model

This section deals with the transient analysis of the tire using a multi body dynamics software, MSC ADAMS [23] which solve equations of statics, quasi-statics, kinematics and dynamics simultaneously and is also capable of running nonlinear dynamics in a tiny fraction of the time required by FEA solutions. Here, in this paper we make three different steady state tire models (corresponding to 20^0C, 40^0C and 60^0C). These steady state tire models are called tire property files. The parameters in this steady state tire models are tuned so that the steady state forces and moments from these models exactly match with the results modified PAC2002 model as described in the previous section. These parameter values are taken from the PAC2002 model explained in the same section. For example with the effect of temperature the value of parameter has changed from Dy to Dy(T).

Since, it is clear from the analysis done by Mizuno et al [20] that the variation of parameter D is due to change in friction at lateral slip corresponding to peak lateral force, therefore, the corresponding sub parameter in ADAMS to be changed to pDy1. The value of pDy1 is tuned such that the value of Dy which we calculate from ADAMS should be equal to the value of Dy(T) from modified PAC2002 model. Similarly other parameters are also tuned in ADAMS. For more details about the parameters, one can refer the reference manual of ADAMS [23]. Figures 9, 10, and 11 show the variation of longitudinal force versus slip ratio, lateral force and self-aligning moment versus slip angle computed from ADAMS. On comparing the results obtained from ADAMS in Figures 9-11 with that from modified PAC2002 model [23] in Figures 6-8, we obtain similar variation corresponding to different temperatures. Now we incorporate these steady state tire models in a demo car model in ADAMS to do the transient analysis at different temperatures. The specification of car and its tires as shown in Figure 12 are mentioned in Table 9. Now, present the transient analysis of tire forces and moment under the condition of acceleration, braking and cornering at different temperatures.

Table 9. Car and tire specifications

Sl. No	Specification	Values	Knits
1	Mass of the car	995	Kg
2	Ixx of the car	2 x 10^8	kg – mm^2
3	Iyy of the car	5 x 10^8	kg – mm^2
4	Izz of the car	6 x 10^8	kg – mm^2
5	Ixy =Iyz =Izx of the car	0 x 10^8	kg – mm^2
7	Mass of the tire	50	kg
8	Ixx of the tire	3.133 x 10^5	kg – mm^2
9	Iyy of the tire	5.8 x 10^5	kg – mm^2
10	Izz of the tire	3.134 x 10^5	kg – mm^2
11	Ixy =Iyz =Izx of the tire	0 x 10^5	kg – mm^2
12	Unloaded tire radius	316.57	Mm
13	Rim radius	186.38	Mm
14	Tire width	185.63	Mm
15	Rim Width	129.11	Mm
16	Aspect Ratio	0.703	-

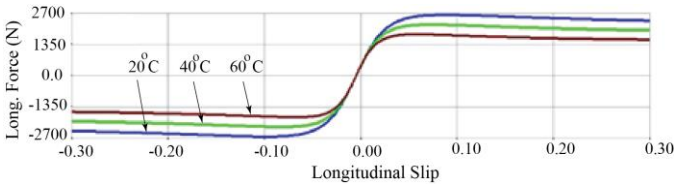

Figure 9: Steady state longitudinal forces at different temperatures

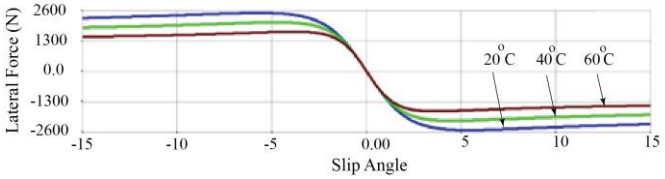

Figure 10. Steady state lateral forces at different temperatures

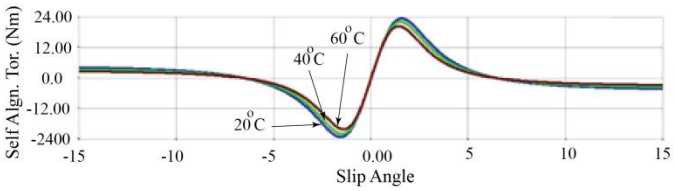

Figure 11. Steady state self-aligning moment at different temperatures

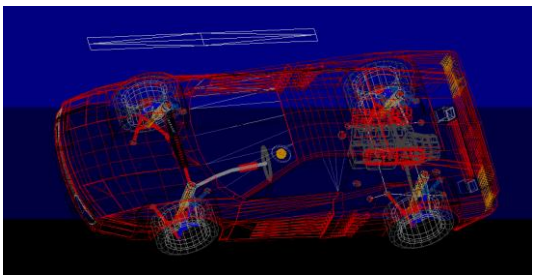

Figure 12: Wire frame model of the demo car in ADAMS

Cornering Analysis

The objective of the cornering analysis in ADAMS is to find the transient response of lateral force and self-aligning moment with respect to slip angles. There are many maneuvering conditions which causes a change in the slip angle. In our analysis, we consider double iso lane change (DLC) maneuver. To do the transient analysis using user defined tire models, the steady state tire property files created at three different temperatures are substituted for the default tire in the ADAMS car separately to form three different analysis. Thus, we will do three different transient analysis corresponding to three different temperatures.

The analysis is done on the car, moving with uniform velocity of 40km/hr and subjected to a DLC maneuver. The step size given is 0.1 and the simulation is done under the third gear. Figures 13 and 14 describe the transient variation of lateral force and self-aligning moment, respectively, at temperatures of 20^oC, 40^oC, and 60^oC. Due to double lane change, it can be seen that the dips/peaks occur when the slip angle changes due to the double lane change incorporated by changing direction of the steering wheel rotation. When the temperature increases, the dip/peak value of lateral force and self-aligning moment decreases. This is because of the decrease in the coefficient of friction with increase in temperature. When rotation of steering wheel changes direction, the lateral slip will be more, and hence, the dip/peak at this point and also the variation of the peak is found to be more as compared that at the first lane change. However, further analysis can be done to observed the influence of temperature dependent tire relaxation length on cornering characteristics.

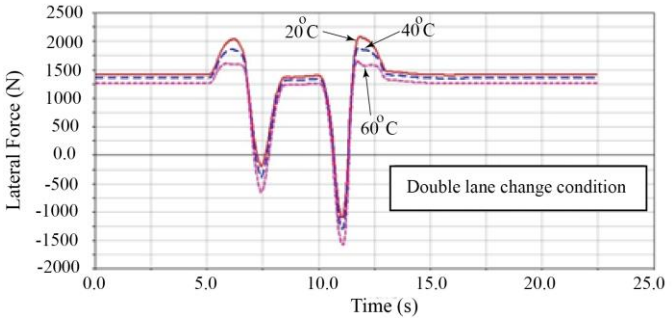

Figure 13. Transient response of lateral force at different temperatures for double ISO lane change maneuver.

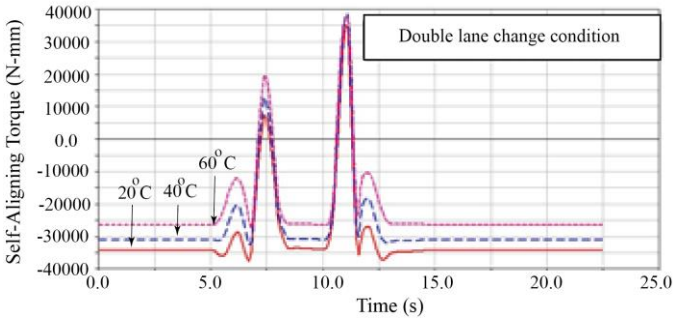

Figure 14. Transient response of self-aligning torque at different temperatures for double ISO lane change maneuver.

Acceleration and Braking Analysis

To study the transient variation of longitudinal forces with respect to slip ratio, we do the acceleration and braking analysis. As explained in the previous section, the steady state tire models at three different temperatures are incorporated in the ADAMS car to do the transient analysis at three different temperatures of 20^oC, 40^oC, and 60^oC.

Acceleration

In order to give an acceleration maneuver, we incorporate the steady state tire model at a particular temperature to the ADAMS car and then perform the simulation. This process is repeated for the three temperatures. To do the analysis, the acceleration is given for a duration of 15 seconds. The throttling is given at time t=1 sec starting from zero to a final throttle of 100 percentage at time t=15 sec. The initial velocity of the car is 10km/hr and step duration is unity. Figure 15 shows the effect of temperature on the longitudinal forces at different temperatures. From the graph, it can be seen that when temperature increases, the longitudinal force decreases after a particular time. It is also noticed that during the constant acceleration, the longitudinal force corresponding to any temperature drops suddenly after certain time probably due to spontaneous increase in longitudinal slip. Under this condition, the tire starts slipping without rolling. As the temperature increases, the time corresponding to the slipping condition without rolling advances as compared to that at lower temperature. This phenomenon occurs primarily due to the decrease in friction with the increase in temperature.

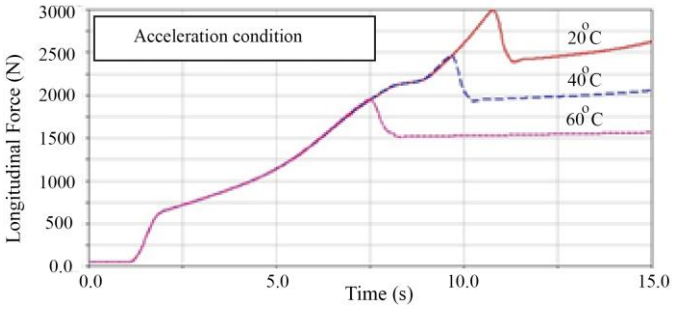

Figure 15. Transient response of longitudinal force at different temperatures during acceleration.

Braking

Similarly, we perform braking analysis to capture the transient response of longitudinal force w.r.t longitudinal slip ratio. Like previous case, we again perform simulations at three different temperatures of 20^oC, 40^oC, and 60^oC by importing the steady state tire models (tire property files) corresponding to three different temperatures in ADAMS. The braking analysis is done on a vehicle moving with initial velocity of 50km/hr. The gear is kept constant at third position and 100 percent brake is applied. The simulation is done for a time period of 10 seconds in 100 steps. Figure 16 shows the variation of longitudinal forces at different temperatures. It can be seen from the graph that when temperature increases, the longitudinal force decreases. Due to decrease in longitudinal force, the wheel get locked earlier than that at lower temperature which makes the wheel slip for a while coming to the rest. The time for which the tire keep on slipping is also found to be larger at higher temperature. This phenomena is again attributed to decrease in friction with temperature. Therefore, at higher temperature, braking condition may induce the instability in the vehicle.

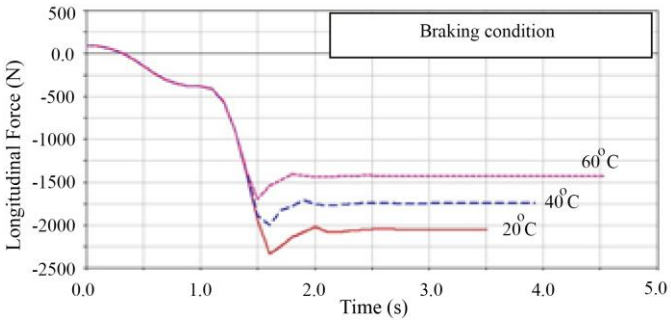

Figure 16. Transient response of Longitudinal Force at different Temperatures during braking

In short, we have found that due to increase in temperature, friction effect between tire and surface reduces. It leads to decrease in lateral and longitudinal forces and self-aligning torque as temperature increases. An interesting observation also found in which the vehicle tire slips without rolling during acceleration and the wheel gets locked early during braking at higher temperature. Since most of effect associated with temperature is localized at the contact region, these effects are mostly neglected while considering the electronic stability control of the vehicle. The analysis presented in the paper may be helpful in improving the stability of high speed vehicle. The modeling of temperature effect on tire dynamics can further be improved by including the effect of tire relaxation length [19].

Conclusions

In this paper, we have studied the steady state and transient response of longitudinal force, lateral force and self-aligning moment under the influence of temperature. To do the analysis, we first present the finite element modeling of tire-surface contact to compute the steady state longitudinal force, lateral force and self-aligning moment. The effect of temperature is modeled in FEM model by taking the appropriate coefficient of friction versus temperature and variation of elastic modulus versus temperature from the literature. After validating the lateral forces computed from FEM model for positive and negative slip angle corresponding to some set of temperature, we numerical obtain the variation of forces and moment versus slip ratio or slip angle at different temperatures. Subsequently, we use the modified PAC2002 model to capture the effect of temperature on tire forces and moment at steady state. On comparing the numerical values of forces and moments with PAC2002 model, we obtain the corresponding empirical parameters, separately for different temperatures. To do the transient analysis of forces and moment at different temperature, we exported the parameters of PAC2002 model to ADAMS. For a car model in ADAMS with standard specification, we analysis the effect of temperature when the car undergoes double lane change condition, acceleration condition and braking condition. We have found that the temperature effect reduces the tire forces and moments. At higher temperature, it may lead to slipping of wheel without rolling under acceleration condition, and early locking of wheel under braking condition. As these conditions are important to maintain the stability of a vehicle, the analysis present in the paper can be very useful in improving the feedback control of electronic stability of the vehicle.

Acknowledgement

AKP would like to acknowledge his students Mr. Shantanu Singh, Mr. Atul Gavade, and Mr. Sagar Tayade for their suggestions during the development of this code. He is also thankful to Prof. Eswaran for encouraging him to work in this area. Finally, the acknowledgement is due to the Institute for giving initial fund for the work.

References

1. Loo, M., " A Model Analysis of Tire behavior Under Vertical Loading and Straight Line Free Rolling," *Tire Science and Technology*. 13(2):67-90, 1985.
2. Davis, D. C, " A Radial-Spring Terrain-Enveloping Tire Model," *Vehicle System Dynamics.* 3:55-69, 1974.
3. Allen, R. W., Magdaleno, R. E., Rosenthal, T. J., Klyde, D. H., et. al, " Modeling Requirements for Vehicle Dynamic Simulation," *Society of Automobile Engineers, SAE Paper.* 950312, 1995.
4. Rotta, J., "Zur Statik des Luftreifens," *Ingenieur-Archiv.* 17, 129-141, 1949.
5. Rhyne, T.B., Cron, S.M., " Development of a non-pneumatic wheel," *Tire Sci. Technol.* 34, 150-169, 2006.
6. Pacejka, H.B, " Tire and Vehicle Dynamics," *Butterworth-Heinemann.* 2002, ISBN 0 7506 5141 5.
7. Dunn, S.E., and Zorowski, C.F., " A study of internal stresses in statically deformed pneumatic tires," *Office of Vehicle Systems Research Contract CST-376, US National Bureau of Standards, Washington, D.C.*, 1970.
8. Ridha, R.A., Satyamurthy, K. and Hirschfelt, L.R., " Finite element modeling of a homogeneous pneumatic tire subjected to footprint loadings," *Tire Sci. Technol.* 13 (2), 91-110, 1985.
9. Chang, J.P., Satyamurthy, K. and Tseng, N.T, " An efficient approach for the three-dimensional finite element analysis of tires," *Tire Sci.Technol.* 16 (4), 249-273), 1988.
10. Faria. L.O., Oden, J.T., Yavari, B., Tworzydlo, W.W.,et. al, " Tire modeling by finite elements," Tire Sci. Technology. 20(1), 33–56, 1992.
11. Danielson, K.T., Noor, A.K., "Analysis of Piston Friction - Effects of Cylinder Bore Temperature Distribution and Oil Temperature," *Tire Sci. Technol.* 25 (1),2–28, 1997.
12. Luchini, J.R. and Popio, J.A., " Modeling transient rolling resistance of tires," *Tire Sci. Technol.* 35 (2), 118-140, 2007.
13. Cho, J.R., Lee, H.W., Jeong, W.B., Jeong , K.M., et. al., " Numerical estimation of rolling resistance and temperature distribution of 3-D periodic patterned tire," International Journal of Solids and Structures. 50, 86–96, 2013.
14. Tian Tang, Daniel Johnson, Emily Ledbury, Thomas Goddette, et al., " Simulation Of Thermal Signature Of Tires and Tracks," *Ground Vehicle Systems Engineering and Technology Symposium (GVSETS).* 2012.
15. Korunovic, N., Trajanivic, M., Stojkovic, M., Misic, D., et. al., " Finite Element Analysis of a Tire Steady Rolling on the Drum and Comparison with Experiment. Journal of Mechanical Engineering," *Journal of Mechanical Engineering.* 57 (12), 888-897, 2011.
16. Bibin S, Atul Gavade, Ashok Kumar Panday., " Dynamic Analysis of Tire Forces and Moment Using Hybrid Approach," *The 22nd International Congress of Sound and Vibration.* 2015.
17. Daniel D. Higgins, Brett A. Marmo, Christopher E. Jeffree, Vasileios Koutsos, et. al., " Morphology of ice wear from rubber–ice friction tests and its dependence on temperature and sliding velocity," *Wear".* 175, 634-644, 2008.
18. Persson, B.N.J., " Rubber friction: role of the flash temperature," *Journal of Physics: Condensed Matter.* 18, 7789–7823, 2006.
19. Angrick, C., van Putten, S., and Prokop, G., "Influence of Tire Core and Surface Temperature on Lateral Tire Characteristics," *SAE Int. J. Passeng. Cars - Mech. Syst.* 7(2):468-481, 2014.
20. Masahiko Mizuno, Hideki Sakai, Kozo Oyama, Yoshitaka Isomura., " The development of the tire side force model considering the dependence of surface temperature of the tire," Vehicle systems dynamics supplement : Taylor and Francis Ltd. 41, 361-370, 2004.
21. Singh, K. B. and Sivaramkrishnan, "An adaptive tire model for enhanced vehicle control systems" S/ *SAE Int. J. Passeng. Cars - Mech. Syst. / Volume 8, Issue 1 (May 2015).*
22. Reference manual, ABAQUS 6.9, [Online.] available: http://www.3ds.com/products-services/simulia/portfolio/abaqus, 2012.
23. Reference manual MSC ADAMS, [Online.] available: http://www.mscsoftware.com/product/adams, 2011.

Contact Information

Contact details for the main author should be included here. Details may include mailing address, email address, and/or telephone number (whichever is deemed appropriate).

Corresponding author

Dr. Ashok Kumar Pandey,
Associate Professor, Mechanical and Aerospace Engineering, Indian Institute of Technology Hyderabad, Kandi, Sangareddy – 502285,
Email: ashok@iith.ac.in